Conf-950401--17

PNL-SA-26298

PROCESSING & PROPERTIES $La_{1-X}A_XCo_{1-Y}Fe_y0_3$(A=Sr, Ca) PEROVSKITES

J. W. Stevenson
T. R. Armstrong
L. R. Pederson
W. J. Weber

April 1995

Presented at the
97th Meeting of American Ceramic Society
April 30 - May 3, 1995
Cincinnati, Ohio

Prepared for
the U.S. Department of Energy
under Contract DE-AC06-76RLO 1830

Pacific Northwest Laboratory
Richland, Washington 99352

DISCLAIMER

This report was prepared as an account of work sponsored by an agency of the United States Government. Neither the United States Government nor any agency thereof, nor any of their employees, makes any warranty, express or implied, or assumes any legal liability or responsibility for the accuracy, completeness, or usefulness of any information, apparatus, product, or process disclosed, or represents that its use would not infringe privately owned rights. Reference herein to any specific commercial product, process, or service by trade name, trademark, manufacturer, or otherwise does not necessarily constitute or imply its endorsement, recommendation, or favoring by the United States Government or any agency thereof. The views and opinions of authors expressed herein do not necessarily state or reflect those of the United States Government or any agency thereof.

DISTRIBUTION OF THIS DOCUMENT IS UNLIMITED

DISTRIBUTION OF THIS DOCUMENT IS UNLIMITED

MASTER

DISCLAIMER

Portions of this document may be illegible in electronic image products. Images are produced from the best available original document.

PROCESSING AND PROPERTIES OF $La_{1-x}A_xCo_{1-y}Fe_yO_{3-\delta}$ (A = Sr,Ca) PEROVSKITES

J.W. Stevenson, T.R. Armstrong, L.R. Pederson, and W.J. Weber
Materials Sciences Department, Pacific Northwest Laboratory†
P.O. Box 999, Richland, WA 99352

ABSTRACT

Selected compositions within the system $La_{1-x}A_xCo_{1-y}Fe_yO_{3-\delta}$ (A=Sr,Ca) were prepared by combustion synthesis and characterized by XRD, TGA, electrical conductivity, and oxygen permeation measurements. Substantial weight loss (due to loss of lattice oxygen) was observed in some compositions at high temperatures. For Sr containing materials, this weight loss increased with increasing Sr content. A substantial decrease in electronic conductivity was observed at high temperatures in Sr doped materials; this decrease was related to the decreased oxygen stoichiometry at these temperatures. In Sr doped compositions, oxygen flux increased with increasing Sr content. Calculated values of ionic conductivity were greater than the conductivity of yttria stabilized zirconia. Substitution of Ca for Sr resulted in substantially lower fluxes.

INTRODUCTION

Compositions in the $(La,Sr)(Co,Fe)O_{3-\delta}$ system with the ABO_3 perovskite-type structure have generated considerable research interest due to their mixed conducting behavior.[1-13] Since, at elevated temperatures, these compositions exhibit substantial anionic and electronic conductivity, they are candidate materials for applications such as solid oxide fuel cell cathodes and oxygen separation membranes. Oxygen anion conductivity in these materials can be quite large relative to other oxygen conductors, such as yttria-stabilized zirconia (YSZ). The mixed conducting behavior results in a spontaneous flux of oxygen through dense sintered materials when they experience an oxygen partial pressure ($P(O_2)$) gradient at elevated temperatures. Under these conditions,

† Operated by Battelle Memorial Institute for the US Department of Energy under contract DE-AC06-76RLO 1830

gaseous oxygen on the high $P(O_2)$ side of the material is reduced to anionic oxygen at the surface, transported through the material (via a lattice vacancy diffusion mechanism) to the low $P(O_2)$ side, and then re-oxidized to O_2. The ionic current resulting from this flux of oxygen ions is offset internally by an electronic current, so that no electrodes or external circuitry are required for the flux to occur.

Teraoka et al[1,2,4] studied the electronic and ionic conductivities of a number of $(La,Sr)(Co,Fe)O_{3-\delta}$ compositions using four-probe dc techniques. At 800°C, ionic conductivities were on the order of 0.01-1 S/cm, while electronic conductivities exceeded 100 S/cm. (Under similar experimental conditions, Kruidhof et al[10] measured the oxygen flux through two of these compositions ($SrCo_{0.8}Fe_{0.2}O_{3-\delta}$ and $La_{0.6}Sr_{0.4}CoO_{3-\delta}$) and obtained values approx. 1 order of magnitude lower than those reported by Teraoka.) Ionic conductivity increased steeply with increasing Sr content and decreased slightly with increasing Fe content. The increase in ionic conductivity with increasing Sr content was attributed to an increase in the concentration of lattice oxygen vacancies as trivalent La cations were replaced by divalent (acceptor) Sr cations. Oxygen permeability was found to be roughly proportional to the ionic conductivity. While compositions with high Sr and Co contents tend to offer the highest oxygen fluxes, other factors must also be considered. For example, $SrCo_{0.8}Fe_{0.2}O_{3-\delta}$ provides very high oxygen permeability but exhibits very limited chemical and structural stability in reduced $P(O_2)$ environments.[5] The purpose of the present study is to increase the understanding of the synthesis and electrochemical properties of materials within the $La_{1-x}A_xCo_{1-y}Fe_yO_{3-\delta}$ (A=Sr,Ca) system in order to facilitate their successful utilization in electrode and oxygen separation applications.

EXPERIMENTAL PROCEDURE

Selected compositions within the system $La_{1-x}A_xCo_{1-y}Fe_yO_{3-\delta}$ (A=Sr,Ca) were prepared using the glycine-nitrate combustion synthesis technique.[14] La, Sr, Ca, Co, and Fe nitrate solutions were mixed in appropriate proportions after which glycine was added as a fuel and complexant. The mixtures were heated in stainless steel beakers until combustion occurred. The resulting ash was calcined at 850°C for 12 h. After calcination, the powders were compacted in a die using uniaxial pressure (55 MPa) followed by isostatic pressure (138 MPa). Green densities were calculated geometrically. Pressed compacts were sintered in $MoSi_2$ furnaces using a heating and cooling rate of 5°C/min; typical sintering temperatures were 1150-1200°C. Relative densities of sintered specimens (as determined by the Archimedes method using ethanol) were greater than 90%. Phase development was determined by X-ray diffraction analysis. Electrical conductivity of sintered specimens was measured in air as a function of temperature (25-1100°C) by a 4-point pulsed dc method. Thermogravimetric analysis was performed on calcined powder specimens using a heating rate of 5°C/min and a cooling rate of 2°C/min. The TGA measurements were performed in several different atmospheres (air; 10,000 ppm O_2 in Ar; 1,000 ppm O_2 in Ar;

100 ppm O_2 in Ar). Passive (i.e., no applied field) oxygen permeation measurements were performed using sintered disc specimens sealed in an alumina test cell with gold gaskets. Air and oxygen were used as source gases with nitrogen as the carrier gas. Permeation was measured as a function of temperature using heating and cooling rates of 0.65°C/min and gas flow rates of 25-30 sccm. An oxygen sensor and mass spectrometer were used in calculating the oxygen fluxes.

RESULTS AND DISCUSSION

Phase Development

For convenience, a simple code is used to refer to the compositions under study. Compositions in the system $La_{1-x}Sr_xCo_{1-y}Fe_yO_{3-\delta}$ are designated by LSCF followed by numerals indicating the relative proportions of each cation. For example, $La_{0.6}Sr_{0.4}Co_{.2}Fe_{0.8}O_{3-\delta}$ is designated LSCF-6428, while $La_{0.2}Sr_{0.8}Co_{.8}Fe_{0.2}O_{3-\delta}$ is LSCF-2882. $La_{1-x}Ca_xCo_{1-y}Fe_yO_{3-\delta}$ compositions are designated LCCF, followed by the numerical code.

Phase development after heat treatment of powders in air at 850°C and 1200°C is summarized in Table I. While the LSCF compositions were essentially single phase perovskites after calcination at 850°C, the LCCF compositions tended to require higher temperature treatment before yielding a high proportion (>95 wt.%) of the desired perovskite phase. The LCCF composition highest in Ca and Co (2882) remained multi-phase even after heating at 1200°C for 2 hours.

Table I. Effect of Temperature on Phase Development (in Air)

Composition	850°C, 12 Hrs	1200°C, 2 Hrs
LSCF-6428	Perovskite	Perovskite
LSCF-4628	99% Perovskite	98% Perovskite
LSCF-4682	Perovskite	99% Perovskite
LSCF-2828	Perovskite	Perovskite
LSCF-2855	99% Perovskite	Perovskite
LSCF-2882	Perovskite	99% Perovskite
LCCF-6428	95% Perovskite	Perovskite
LCCF-4628	85% Perovskite	95% Perovskite
LCCF-4682	80% Perovskite	95% Perovskite
LCCF-2882	35% Perovskite	75% Perovskite

Thermogravimetric Analysis

TGA results for the LSCF compositions when heated and cooled in air are shown in Figure 1. These materials exhibited a substantial weight loss at elevated temperatures; this weight loss was reversible upon cooling. (In some specimens, a slight irreversible weight loss was observed during the early stages of heating

due to the removal of moisture in the powder. To avoid confusion, this transient behavior is not shown in the plots). The weight loss upon heating was due to a partial loss of lattice oxygen, so that the oxygen deficiency, δ, increased with increasing temperature. The temperature at which oxygen loss began to occur was highly dependent on the composition, with oxygen loss beginning to occur at lower temperatures as the Sr content increased. The magnitude of the oxygen loss increased with increasing Sr content. Similar weight loss behavior was previously reported by Tai et al[8] for two of these compositions (LSCF-6428,4628).

TGA measurements were also performed in various atmospheres to study the effect of ambient $P(O_2)$ on weight loss behavior. Figure 2 shows the behavior of a high cobalt composition (LSCF-2882) in a variety of ambient oxygen partial pressures. The magnitude of the oxygen loss upon heating increased only slightly as the ambient $P(O_2)$ was reduced. In 10,000 ppm O_2, full re-oxidation was observed upon cooling (as in air), but re-oxidation did not occur in atmospheres of 1,000 and 100 ppm O_2. Compositions containing less cobalt did not experience full re-oxidation in the 10,000 ppm O_2 environment. For a given Sr content (e.g., x = 0.6, 0.8), the degree of re-oxidation during cooling in the 10,000 ppm O_2 atmosphere decreased with increasing substitution of Fe for Co (See Figure 3).

Electrical conductivity

Since the ionic transport number in these compositions is less than 1%, the bulk conductivities obtained by the 4-probe measurements can be considered to represent the electronic conductivities of the materials. Plots of log σT vs. 1000/T (σ is conductivity and T is absolute temperature) for the LSCF compositions are shown in Figure 4. At lower temperatures, conductivities tended to increase with increasing temperature, with activation energies on the order of 0.05-0.16 eV (Table II). These energies are similar to magnitude to activation energies reported for compositions in $(Y,Ca)MnO_3$,[16,17] $(La,Ca)MnO_3$,[16] $(La, Sr)MnO_3$,[18] and $(La,Sr)CrO_3$.[19] This behavior is consistent with a small polaron conduction mechanism (i.e., localized electronic carriers having a thermally activated mobility).

If the carrier concentration is constant, small polaron conduction follows the relation:[19]

$$\sigma T = C \exp(-E_a/kT) \qquad [1]$$

where E_a is the activation energy, and k is the Boltzmann constant. The pre-exponential factor C is a constant which includes the carrier concentration as well as other material dependent parameters.

At higher temperatures, conductivity was observed to decrease substantially with increasing temperature. Figure 5 shows conductivity as a

Table II. Activation Energies for Electronic Conduction

Composition	Activation Energy (eV)	Ref.
LSCF-6428	0.079	
LSCF-4628	0.075	
LSCF-2882	0.051	
LSCF-2828	0.089	
LCCF-6428	0.154	
LCCF-4628	0.159	
LCCF-4682	0.099	
(Y,Ca)MnO_3	0.04-0.23	16
(Y,Ca)MnO_3	0.05-0.37	17
(La,Ca)MnO_3	0.08-0.15	16
(La,Sr)MnO_3	0.09-0.19	18
(La,Sr)CrO_3	0.11-0.19	19

function of temperature for LSCF-6428. The symbols represent the experimental results. The dashed line represents the expected behavior for small polaron conduction with a constant concentration of charge carriers (calculated using Eq. 1). It is obvious that the conductivity decreased at high temperatures much more rapidly than predicted by the model. This exaggerated decrease at high temperatures can be attributed to a decreasing concentration of electronic charge carriers (electron holes, $h^{\bullet}$) as the oxygen content of the material decreases. This process can be represented (Kroger-Vink notation)[20] as:

$$2h^{\cdot} + O_O^x \Rightarrow V_O^{\cdot\cdot} + \tfrac{1}{2}O_2 \qquad [2]$$

Thus, two electron holes are eliminated for each oxygen ion leaving the lattice. Accordingly, the conductivity model was modified to allow for a variable carrier concentration:

$$\sigma T = \{(A' - 2\delta)(1-(\delta/2))\ C'\}\exp(-E_a/kT) \qquad [3]$$

Two new terms were included in the pre-exponential factor. The first represents the temperature dependent carrier concentration. In perovskites, electronic conduction occurs on the BO_3 sublattice.[21] If each new oxygen vacancy eliminates two electron holes, the initial concentration of carriers (A') created by the acceptor (i.e., Sr or Ca) doping on the A site is reduced at elevated temperatures by 2δ, where δ is the temperature dependent oxygen vacancy concentration (as calculated from the TGA measurements). The second term in the pre-exponential factor represents the decrease in hole mobility due to the introduction of oxygen vacancies.[16] Since the transport of carriers between adjacent B-site cations occurs via an exchange interaction involving the oxygen

anions between those cations, electron transfer does not occur between cations separated by oxygen vacancies.

The solid line represents the calculated conductivity obtained from Eq. 3. This line provides a good fit to the experimental data, supporting the conclusion that the substantial decrease in conductivity at high temperatures is indeed due to the mechanism described in Eq. 2. It should be noted that while this decrease in oxygen stoichiometry with increasing temperature reduces the concentration of electronic carriers, it simultaneously results in an increase in the concentration of the ionic charge carriers (oxygen vacancies).

Unlike the LSCF compositions, the LCCF compositions did not exhibit the pronounced decline in conductivity at elevated temperatures (Figure 6). The plots of σT vs. 1000/T are relatively linear over the entire temperature range, indicating that the electronic carrier concentrations in these materials remain nearly constant. This behavior implies that the oxygen stoichiometry in the LCCF compositions is essentially independent of temperature. This conclusion is supported by the TGA data for LCCF-4628, which showed minimal weight change throughout the temperature range studied (See Figure 7; for comparison, the TGA data for LSCF-4628 is also shown).

Oxygen permeation

Oxygen permeation rates (oxygen vs. nitrogen) through sintered specimens of several LSCF and LCCF compositions (2.3 - 3.1 mm thick) are shown as a function of temperature in Figure 8. In the LSCF compositions, increased Sr content results in a substantial increase in flux. This is consistent with the TGA results which demonstrated that, at high temperatures, the degree of oxygen deficiency increases with increasing Sr content. The rapid increase in oxygen flux with increasing temperature can be attributed to two factors: an increasing mobility of the lattice oxygen ions, and an increasing concentration of lattice oxygen vacancies. Fluxes measured in air vs. nitrogen tended to be substantially lower than those measured in oxygen vs. nitrogen (as shown in Figure 9 for LSCF-4628) due to the reduced $P(O_2)$ gradient.

Fluxes for the LCCF compositions were significantly lower than for the LSCF compositions, as would be expected since the oxygen stoichiometry of these materials appears to be relatively independent of temperature (Figure 7), so that an enhancement in oxygen vacancy concentration does not occur at high temperatures.

Ionic conductivities were calculated from the flux rates, using the relation:[22]

$$\sigma_i = \frac{4 F J t}{R T \ln\left[P(O_2^I)/P(O_2^{II})\right]} \qquad [4]$$

where F is Faraday's constant, J is flux (in A/cm^2), t is specimen thickness, R is the gas constant, T is absolute temperature, and $P(O_2^I)$ and $P(O_2^{II})$ are the oxygen partial pressures on each side of the specimen. The calculated values of ionic conductivity for the LSCF compositions at 900°C (see Table III) are higher than the conductivity of YSZ at that temperature (approx. 0.1 S/cm). These values are similar in magnitude to conductivities measured with a 4-probe dc technique by Teraoka et al.[2] Ionic transport numbers were obtained by dividing the ionic conductivity by the total conductivity.

CONCLUSIONS

LSCF compositions exhibited a substantial reversible weight loss at elevated temperatures when heated in air due to a partial loss of lattice oxygen. As Sr content increased, the oxygen loss began to occur at lower temperatures and the magnitude of the oxygen loss increased. Bulk electronic behavior was consistent with the small polaron conduction mechanism. A substantial decrease in bulk conductivity was observed at elevated temperatures; this behavior was attributed to a decrease in electronic charge carriers resulting from the decrease in oxygen stoichiometry. Unlike the LSCF compositions, LCCF compositions did not exhibit a substantial decrease in conductivity at high temperatures. Oxygen flux through sintered LSCF specimens increased with increasing Sr content. Fluxes through LCCF specimens were approximately 1 order of magnitude lower than fluxes measured through LSCF materials. Calculated values of ionic conductivity for the LSCF compositions at high temperatures were significantly greater than that of YSZ.

Table III. Ionic and Electronic Conductivities at 900°C

Composition	Ionic Conductivity (S/cm)	Electronic Conductivity (S/cm)	Ionic Transport Number
LSCF-6428	0.23	252	9.1×10^{-4}
LSCF-4628	0.40	219	1.8×10^{-3}
LSCF-2828	0.62	120	5.2×10^{-3}
LSCF-2882	0.87	310	2.8×10^{-3}
LCCF-4628	0.03	52	5.8×10^{-4}
LCCF-4682	0.01	296	3.4×10^{-5}

ACKNOWLEDGMENTS

The authors thank Ron Stephens, David McCready, Stephen Vahey, and Robert Carneim for their assistance with this work. The financial support of the Department of Energy's Fossil Energy AR&TD Materials Program is gratefully acknowledged.

REFERENCES

1. Y. Teraoka, H. Zhang, S. Furukawa, and N. Yamazoe, "Oxygen Permeation through Perovskite-Type Oxides," Chemistry Letters, 1743-1746 (1985).
2. Y. Teraoka, H. Zhang, K. Okamoto, and N. Yamazoe, "Mixed Ionic-Electronic Conductivity of $La_{1-x}Sr_xCo_{1-y}Fe_yO_{3-\delta}$ Perovskite-Type Oxides," Mat. Res. Bull., **23**, 51-58 (1988).
3. S. Sekido, H. Tachibana, Y. Yamamura, and T. Kambara, "Electric-Ionic Conductivity in Perovskite-Type Oxides, $Sr_xLa_{1-x}Co_{1-y}Fe_yO_{3-\delta}$," Solid State Ionics, **37**, 253-259 (1990).
4. Y. Teraoka, T. Nobunaga, K. Okamoto, N. Miura, and N. Yamazoe, "Influence of Constituent Metal Cations in Substituted $LaCoO_3$ on Mixed Conductivity and Oxygen Permeability," Solid State Ionics, **48**, 207-212 (1991).
5. U. Balachandran, S. Morissette, J. Picciolo, J. Dusek, and R. Peoppel,"Fabrication of Ceramic Membrane Tubes for Direct Conversion of Natural Gas," Proc. International Gas Research Conference, Ed. H. Thompson, Government Institutes, Rockville, MD, pp. 565-573 (1992).
6. S. Carter, A. Selcuk, R. Chater, J. Kajda, J. Kilner and B. Steele, "Oxygen Transport in Selected Nonstoichiometric Perovskite-Structure Oxides," Solid State Ionics, **53-56**, 597-605 (1992).
7. B. Steele, "Oxygen ion conductors and their technological applications," Mat. Sci. and Eng., **B13**, 79-87 (1992).
8. L. Tai, M. Nasrallah, and H. Anderson, "$(La_{1-x}Sr_x)(Co_{1-y}Fe_y)O_3$, A Potential Cathode for Intermediate Temperature SOFC Applications," Proc. 3rd Int. Symp. on SOFC, Electrochem. Soc., Vol. 93-4, 241-251 (1993).
9. H. Anderson, C. Chen, L. Tai, and M. Nasrallah, "Electrical Conductivity and Defect Structure of $(La,Sr)(Co,Fe)O_3$," Proc. 2nd Int. Symp on Ionic and Mixed Conducting Ceramics, Ed. T. Ramanarayanan, W. Worrell, and H. Tuller, Electrochem. Soc., Vol. 94-12, 376-387 (1994).
10. H. Kruidhof, H. Bouwmeester, R. v. Doorn, and A. Burggraaf, "Influence of Order-Disorder Transitions on Oxygen Permeability through Selected Nonstoichiometric Perovskite-Type Oxides," Solid State Ionics, **63-65**, 816-822 (1993).
11. H. Bouwmeester, H. Kruidhof, and A. Burggraaf, "Importance of the Surface Exchange Kinetics as Rate Limiting Step in Oxygen Permeation through Mixed-Conducting Oxides," Solid State Ionics, **72**, 185-194 (1994).
12. U. Balachandran, J. Dusek, S. Sweeney, R. Peoppel, R. Mieville, P. Maiya, M. Kleefisch, S. Pei, T. Kobylinski, C. Udovich, and A. Bose,"Methane to Syngas via Ceramic Membranes," Am. Cer. Soc. Bulletin, **74**, 71-75 (1995).
13. C.C. Chen, M.M. Nasrallah, H.U. Anderson, and M.A. Alim, "Immittance Response of $La_{0.6}Sr_{0.4}Co_{0.2}Fe_{0.8}O_3$," J. Electrochem. Soc., **142**, 491-496 (1995).
14. L.A. Chick, L.R. Pederson, G.D. Maupin, J.L. Bates, L.E. Thomas, and G.J. Exarhos, "Glycine-Nitrate Combustion Synthesis of Oxide Ceramic Powders," Materials Letters, **10**, 6-12 (1990).

15. R. Nadalin and W. Brozda, "Chemical Methods for the Determination of the Oxidizing (or Reducing) Power of Certain Materials Containing a Multivalent Element in Several Oxidation States," Analytica Chimica Acta, **28**, 282-293 (1963).
16. J.W. Stevenson, M.M. Nasrallah, H.U. Anderson, and D.M. Sparlin, "Defect Structure of $Y_{1-y}Ca_yMnO_3$ and $La_{1-y}Ca_yMnO_3$ I. Electrical Properties, II. Oxidation-Reduction Behavior," J. Solid State Chem., **102**, 175-197 (1993).
17. J. Bates, T. Armstrong, L. Chick, W. Weber, C. Windisch, and G. Youngblood, Gas Research Institute, Contract 5088-294-1707 Final Report, p. 68 (1993).
18. J.H. Kuo, H.U. Anderson, and D.M. Sparlin, "Oxidation-Reduction Behavior of Undoped and Sr-Doped $LaMnO_3$: Defect Structure, Electrical Conductivity, and Thermoelectric Power," J. Solid State Chem., **87**, 55-63 (1990).
19. D. P. Karim and A.T. Aldred, "Localized Level Hopping Transport in $La(Sr)CrO_3$," Phys. Rev. B, **20**, 2255-2263 (1979).
20. F.A. Kroger, The Chemistry of Imperfect Crystals, North-Holland, Amsterdam (1964).
21. J.B. Goodenough, "Metallic Oxides," Prog. Inorg. Chem., **5**, 145-399, Pergamon Press, New York, (1971).
22. M. Liu and A. Joshi, "Characterization of Mixed Ionic-Electronic Conductors," Proc. First Int. Symp. Ionic and Mixed Conducting Ceramics, Eds. T.A. Ramanarayanan and H.L. Tuller, Electrochem. Soc, Proc. Vol. 91-12, 231-246 (1991).

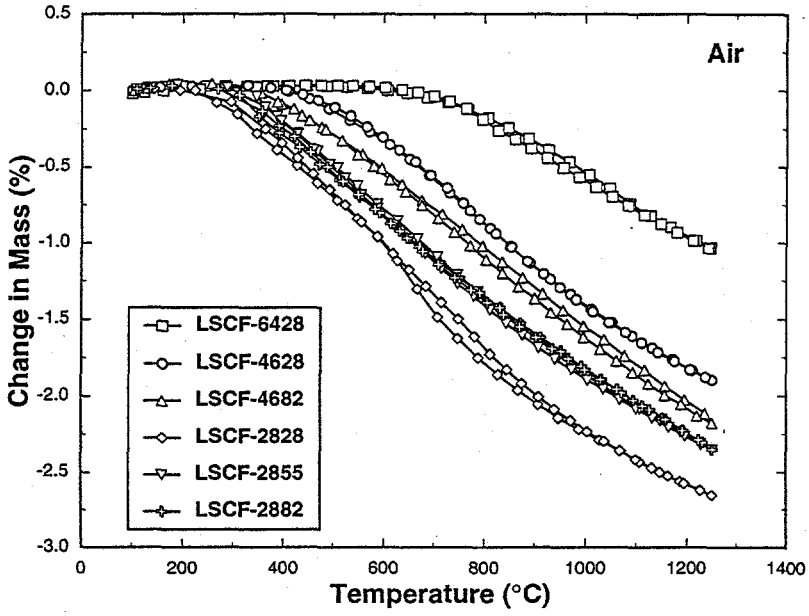

Figure 1. Thermogravimetric measurements on LSCF compositions in air.

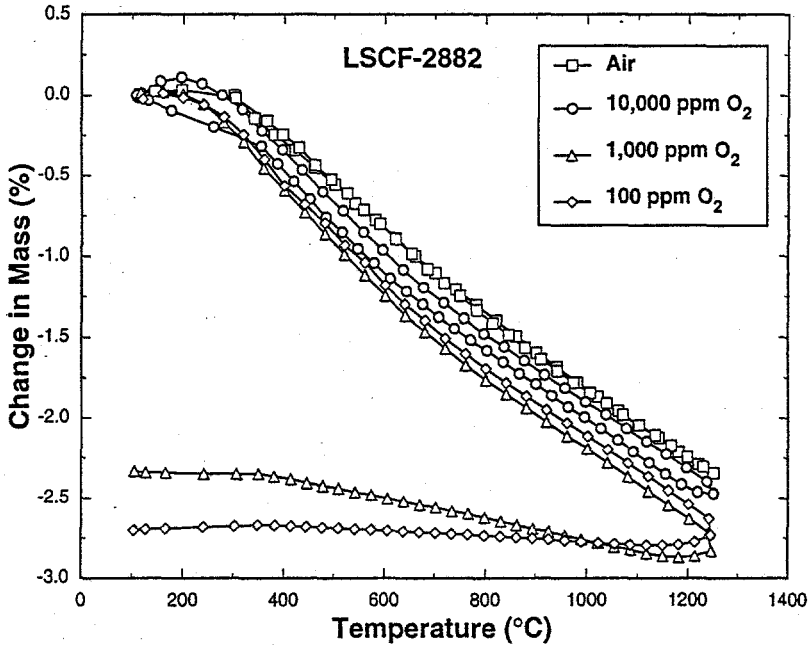

Fig. 2. Thermogravimetric measurements on LSCF-2882 in various atmospheres.

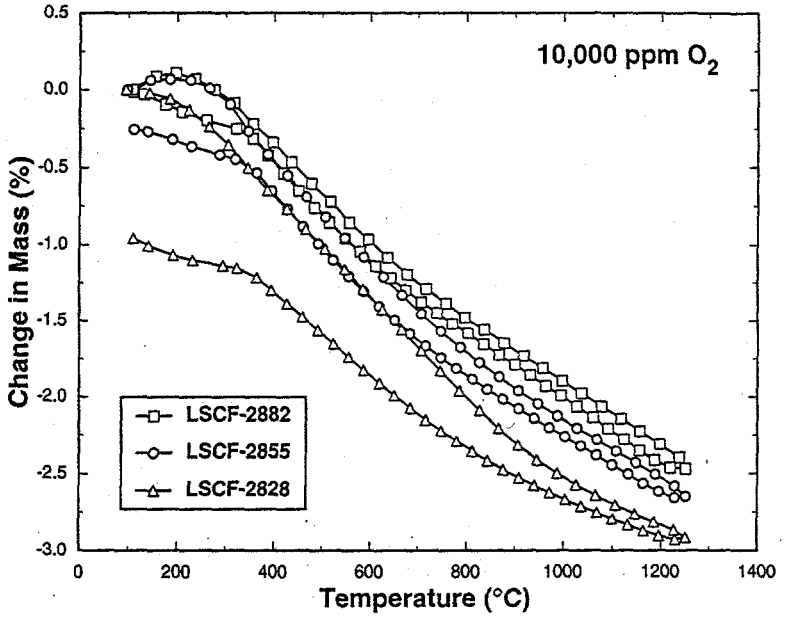

Fig. 3. Thermogravimetric measurements on LSCF-2828, 2855, 2882 in 10,000 ppm O_2.

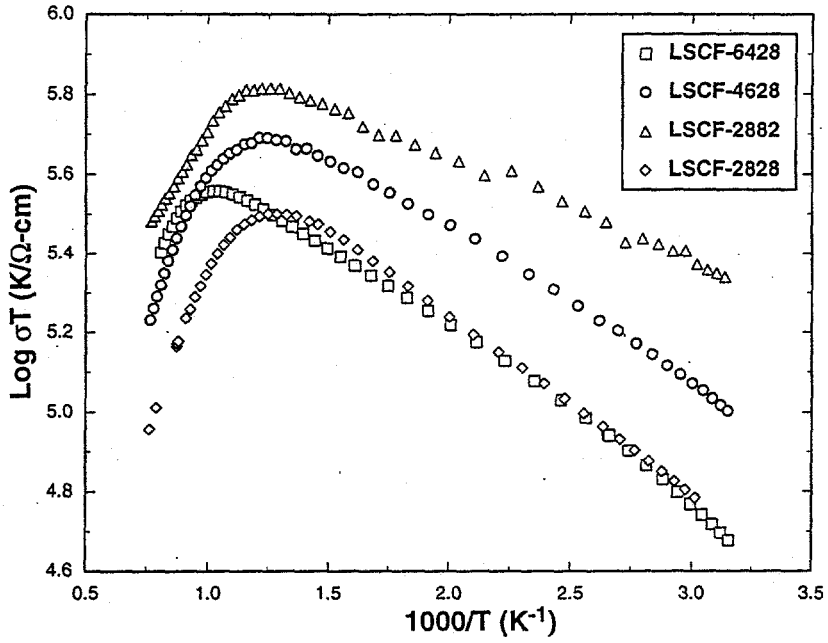

Fig. 4. 4-probe dc conductivity data for the indicated LSCF compositions.

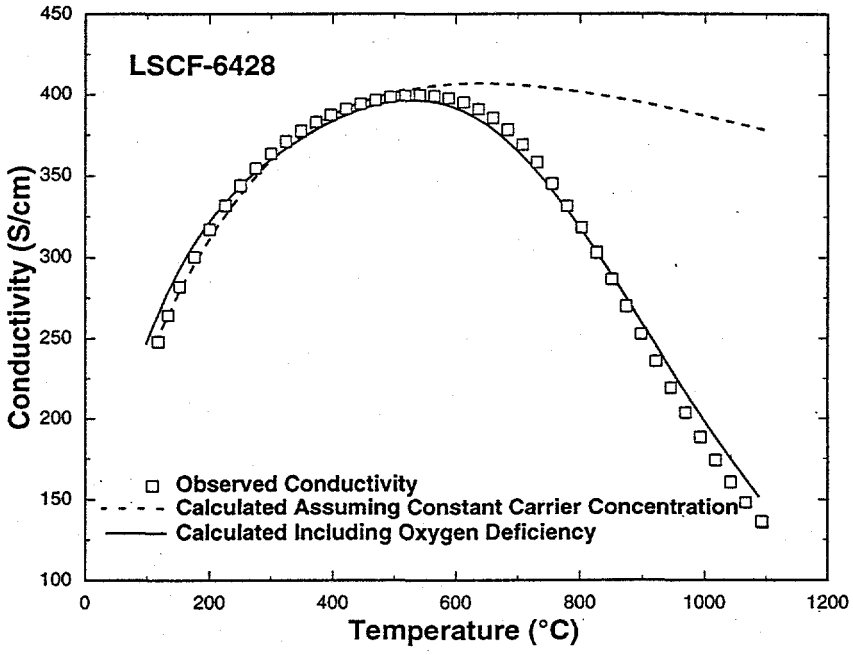

Fig. 5. Electrical conductivity of LSCF-6428 as a function of temperature.

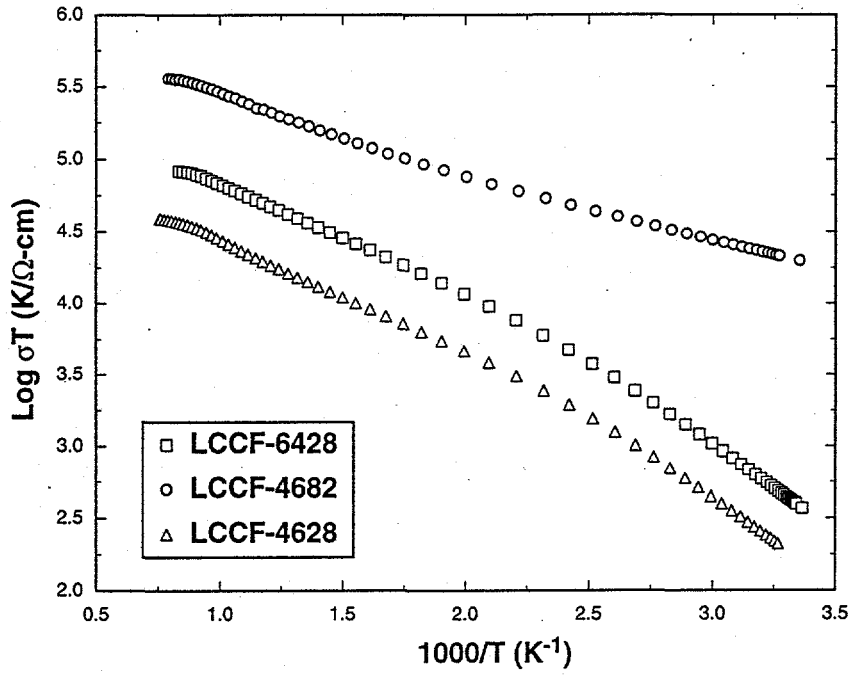

Fig. 6. 4-probe dc conductivity data for the indicated LCCF compositions.

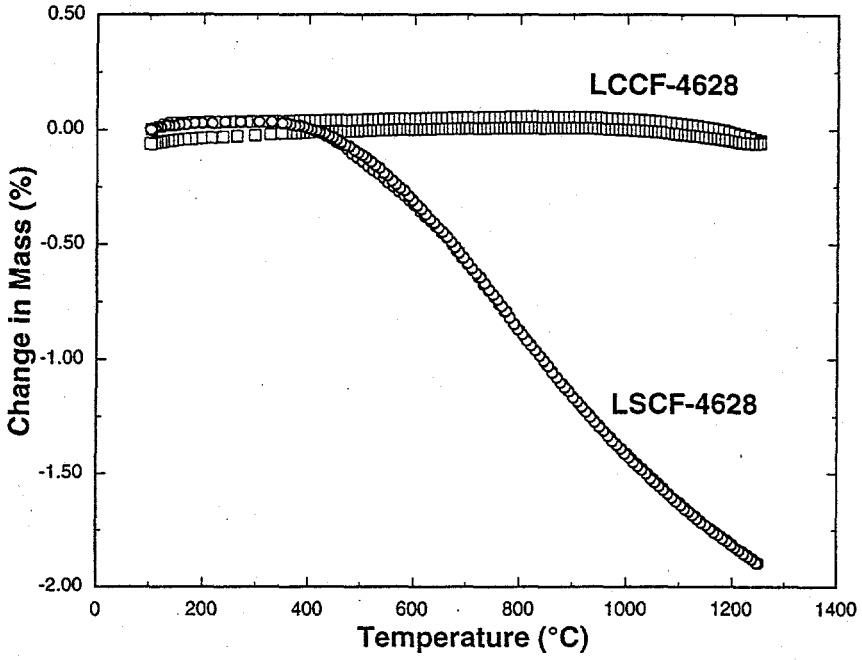

Fig. 7. Thermogravimetric measurements on LCCF-4628 and LSCF-4628.

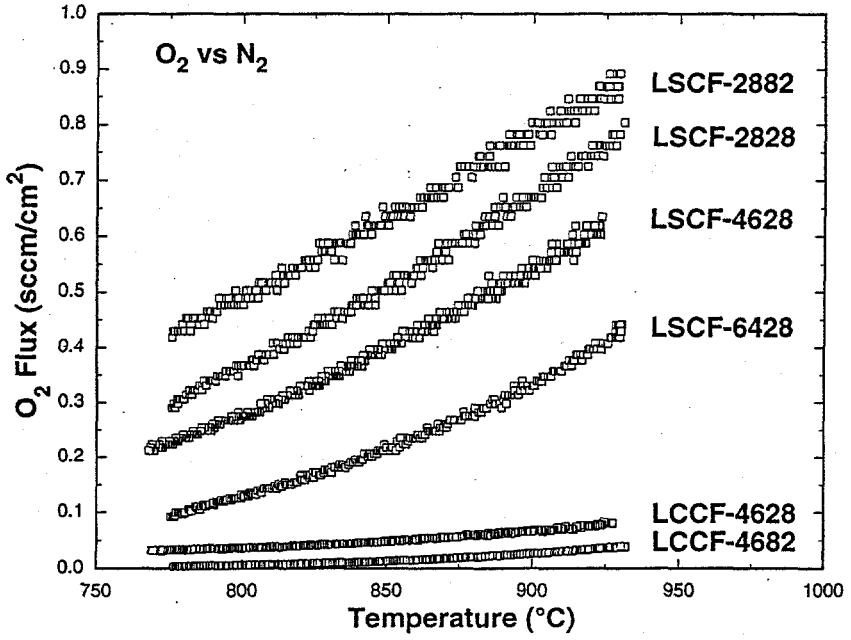

Fig. 8. Oxygen permeation measurements (O_2 vs N_2) on sintered specimens of the indicated compositions.

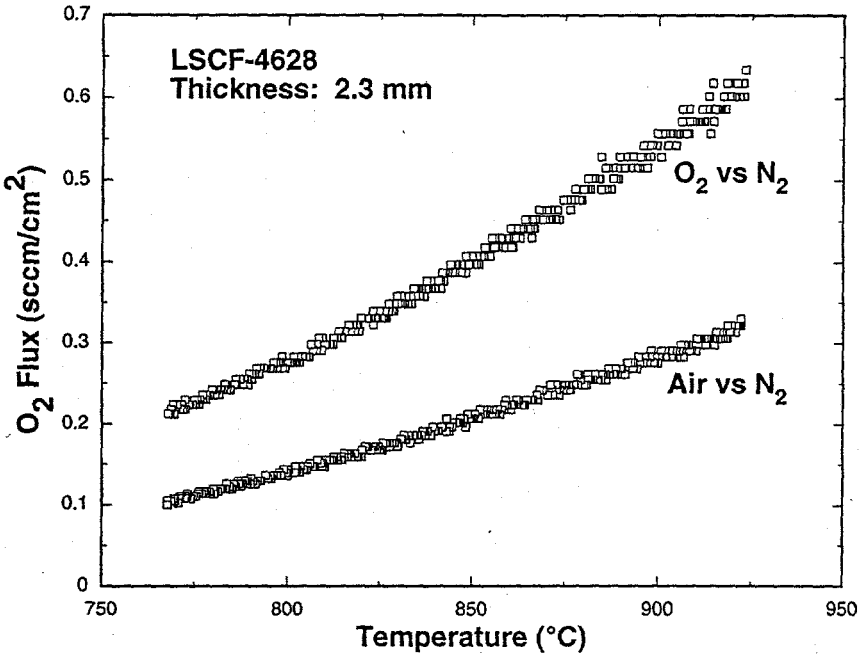

Fig. 9. Oxygen permeation measurements on LSCF-4628 in O_2 vs N_2 and in air vs N_2.